

## Effect of the surface track potential on electron emission in 60–100 keV $H^+$ grazing bombardment of LiF

G. R. Gómez, O. Grizzi,\* E. A. Sánchez,\* and V. H. Ponce

*Centro Atómico Bariloche, Comisión Nacional de Energía Atómica, 8400-S.C. de Bariloche, Argentina*

(Received 1 April 1998)

We have measured energy distributions of electrons emitted at forward angles during 60–100 keV  $H^+$  grazing bombardment of LiF surfaces. The electron energy spectra from the insulator are compared with those for Al(111), Si(111), and gas phase Ar. In the case of LiF, a broad peak appears with the maximum at an energy  $E_m$  lower than the convoy electron energy ( $E_{ce}$ ). The absolute value of the energy shift  $\Delta E = E_m - E_{ce}$  increases with the  $H^+$  velocity, and depends on the sample topography. The results are discussed in terms of the attractive (track) and the repulsive surface-induced potentials. [S0163-1829(98)00132-5]

The electron emission induced by ion bombardment of insulating surfaces differs markedly from that of metals or semiconductors.<sup>1</sup> It is affected by the low density of conduction electrons and the large band gap, which result in the increase of the secondary-electron mean-free path and in the macroscopic charging up of the sample.<sup>1,2</sup> Measurements of electron emission are scarce for insulators; this is partly due to the experimental difficulties raised from the preparation and charging up of the samples. The LiF surface has the advantage of being a good ionic conductor at temperatures above 350 °C, and at this temperature its surface can be prepared *in situ* by grazing ion bombardment and annealing.<sup>3</sup> Most of the previous works on insulators were performed at large incident and observation angles.<sup>1,2,4,5</sup> The grazing experimental geometry used in this work enhances the surface sensitivity, and allows a simple description of the ion trajectory. In this letter we present the first measurements of the forward electron energy distributions resulting from grazing proton bombardment of an insulating (LiF) surface.

In grazing collisions of fast ions with rough metallic and semiconductor surfaces the electron emission in the region of the specularly reflected beam presents a strong peak centered at an energy  $E_{ce} = (m_e/M_p)E_p$  (where  $m_e$  and  $M_p$  are the electron and ion masses, and  $E_p$  the projectile energy),<sup>6</sup> usually referred to as the convoy peak. For sufficiently smooth surfaces, such as those obtained by prolonged cycles of grazing ion bombardment and annealing, the electron emission intensity at  $E_{ce}$  is strongly reduced, and a peak appears at an energy  $E_m$  higher than  $E_{ce}$ .<sup>7–10</sup> This behavior has been ascribed to the screening of the coulombic ion potential by the surface induced potentials ( $V_{ind}$ ),<sup>11</sup> and the accelerating effect produced by  $V_{ind}$  on the convoy electrons.<sup>7,8</sup> More recently Reinhold *et al.*,<sup>12</sup> based on a Monte Carlo calculation, related the structure at  $E_m$  to a rainbow effect produced by  $V_{ind}$ . In the intermediate and low projectile energy regime, where  $\Delta E = E_m - E_{ce}$  and  $V_{ind}$  present different behavior with  $E_p$ ,<sup>9,10</sup> a theoretical description is not yet available. If instead of a metal or a semiconductor surface, an insulator is used, one can expect qualitative changes in the forward-electron energy distribution due to the differences in the electronic structure. As a consequence of the low conductivity, there is a reduction in the dynamic response of the sur-

face and, in addition, the emitted electrons may be affected by the track potential, resulting from the target ionization produced along the ion path. The existence of such effects might be useful for getting direct information of the surface track potential, which is poorly known at present.

The measurements were performed in a previously described UHV chamber equipped with facilities for Auger-electron spectroscopy (AES), sample sputtering, and annealing. The mass-analyzed  $H^+$  beam was accelerated to 60–100 keV and collimated to  $\phi 1$  mm. All the spectra were acquired with a resolution of 1%, an acceptance angle of  $\pm 0.7^\circ$ , and were corrected for the transmission function of the analyzer. Two single crystals of LiF were prepared by repeated cycles of 22 keV  $Ar^+$  grazing bombardment with the surface held at 350 °C, and annealing at 400 °C. The first sample, which we will refer to as A, was previously bombarded with 500 eV of  $Ar^+$  at an incidence of  $45^\circ$  to remove the oxygen contamination detected with AES (performed in a pulse-counting mode to reduce electron bombardment). The second surface (B) was cleaved in air and immediately placed in the UHV chamber. For this sample the grazing ion bombardment and annealing cycles were sufficient to remove the initial contamination, so no sputtering at large angles was performed. We characterized the topography of both LiF surfaces using an atomic force microscope (AFM) operating in air. The root-mean-square (rms) deviation of the height distribution of sample A ( $\sim 67.6$  Å) was greater than that of B ( $\sim 25.5$  Å), and presented more smooth terraces, typically of more than 100 Å long, where the grazing ions could be reflected specularly.

We made a preliminary study in order to determine the experimental conditions that prevent macroscopic charging up of the sample. For beam currents ( $I_c$ ) in the 5–20 nA range, despite the high temperature of the surface ( $T_s \sim 400$  °C), the electron energy distributions below 30 eV were dependent on both  $I_c$  and the bombarding time. We observed that by reducing  $I_c$  to  $\sim 2$  nA, the shape of the spectra became reproducible and independent of both the bombarding time and  $I_c$ . Based on this result,  $I_c$  was set to 0.5–1 nA, with  $T_s \sim 400$  °C, for all the measurements.

In Fig. 1(a) we present the energy distribution of the electrons ejected along the direction of the ion specular reflection

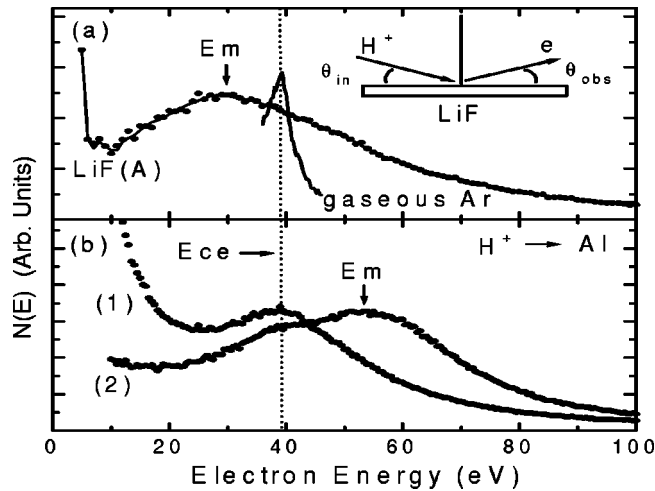


FIG. 1. (a) Electron energy distribution measured during 70 keV  $H^+$  grazing bombardment of LiF sample A. The experimental geometry is shown in the inset. Full line spectrum: electron transfer to the continuum peak in 70 keV  $H^+$ -Ar(gas) collisions. (b) The same as (a) for a rough (1) and a flat (2) Al surface.

for 70 keV  $H^+$  collisions with LiF surface A. The incidence direction was set at  $\theta_{in} = 1.5^\circ$  with respect to the surface plane, randomly oriented. The figure also shows an electron energy distribution measured for 70 keV  $H^+$ -Ar collisions. The spectrum from LiF shows a broad peak with its maximum at an energy  $E_m < E_{ce}$ . We measured several spectra for  $E_p$  varying from 60 keV to 100 keV, and keeping the other experimental conditions fixed. We found that the shift  $\Delta E = E_m - E_{ce}$  increases with the ion energy (it changes from  $-5$  eV at 60 keV to  $-13$  eV at 100 keV). This shift cannot be ascribed to the surface stopping power, which reduces the projectile energy only by  $\sim 1\%$ . The electron energy distributions measured at  $E_p < 60$  keV and  $\theta_{in} < 1.5^\circ$  showed a strong intensity reduction. This effect was attributed to the increase of the impact parameters and the associated decrease of the surface ionization.

In order to make a comparison with results obtained for metal samples, we present in Fig. 1(b) two energy distributions of electrons ejected during 70 keV  $H^+$  grazing bombardment of Al. The incidence and observation angles are the same as in Fig. 1(a). The Al spectra were measured: (1) after cleaning the surface with Ar sputtering at a large incidence angle, and (2) after performing many cycles (about two weeks) consisting of grazing 20 keV  $Ar^+$  bombardment and subsequent annealings to improve the surface flatness.<sup>13,14</sup> With the AFM we were able to confirm that distribution (1) corresponds to electrons emitted from a rough surface, whereas (2) comes from a smoother one.<sup>14</sup> All the forward electron energy distributions measured for non-insulating samples show a similar behavior, i.e., for rough surfaces there is a prominent convoy peak<sup>9</sup> (spectrum 1), while a peak at  $E_m \geq E_{ce}$  (spectrum 2) is normally observed for surfaces with smooth regions of at least 100 Å long.<sup>14</sup> Although the intensity and position of the structure at  $E_m$  change for different samples, the energy position of its maximum is (in contrast to what is observed in LiF) always higher than or equal to  $E_{ce}$  for all the semiconductors and metals studied.

Previous results<sup>2,3,5</sup> show that the yield of secondary elec-

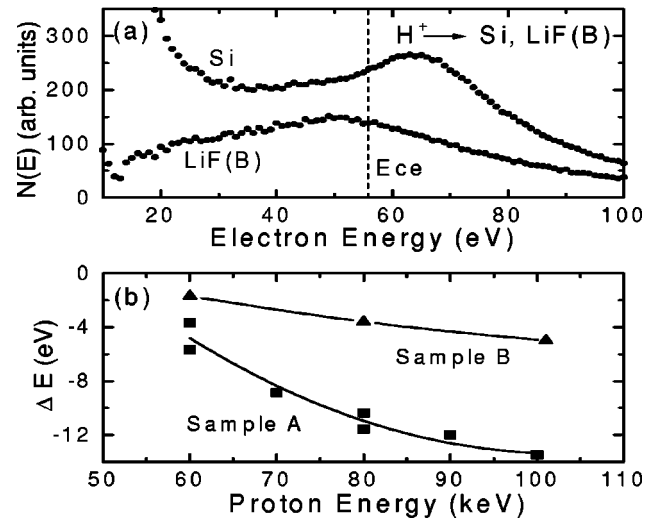


FIG. 2. (a) Energy spectra of electrons emitted at  $\theta_{obs} = \theta_{in} = 1.5^\circ$  in 100 keV  $H^+$  grazing collisions with Si and LiF (sample B) surfaces. The spectra are normalized to the incoming beam current and for the different sample size. (b) Energy shift  $\Delta E = E_m - E_{ce}$  as a function of the  $H^+$  energy for LiF samples A and B.

trons emitted during ion bombardment of insulating surfaces can be higher than that observed with noninsulating surfaces for the same bombardment conditions. In order to compare the intensity of the electrons emitted at forward angles from LiF with results for noninsulating surfaces, we placed the LiF sample B and a Si single crystal in the same sample holder. This allowed us to measure both surfaces under the same experimental conditions (beam current, incident and observation angles, detector efficiency). The results for 100 keV  $H^+$  are shown in Fig. 2(a). We can see that the peak at  $E_m$  is broader for LiF and, as seen for sample A, the electron energy distribution coming from the insulator has a maximum at  $E_m < E_{ce}$ . If we compare the counts at  $E_m$  after linear background subtraction and correction for different sample size, the opposite shifted structures have similar intensities. The background of secondary electrons is reduced in intensity for LiF. This is not necessarily in disagreement with previous measurements at large incidence angles. The energy distributions of secondary electrons emitted in noble gas ion bombardment of LiF show that  $\sim 95\%$  of the emitted electrons have energies lower than 10 eV,<sup>4</sup> where we also observe an increment of the counts [Fig. 1(a)]. In addition, the electron emission intensity at low observation angles is possibly reduced for an insulator because many low-energy electrons could be attracted back to the surface by the track potential. With LiF sample B we also observed an increase in the absolute value of  $\Delta E$  with  $E_p$ , but the shifts turned out to be smaller than those measured for sample A [Fig. 2(b)]. As it will be discussed later, we attribute the difference in  $\Delta E$  to the different topography of surfaces A and B.

We can summarize the main features of the electron emission from LiF that contrast with the results for noninsulating samples: at observation angles in the region of the specularly reflected beam, the spectrum shows a prominent structure at an energy  $E_m < E_{ce}$ . The position of this structure depends on the topography, with  $\Delta E$  being larger for a rough surface. From the measured angular distributions (not shown in the paper) we observed that the shifted structure appears in a

broad region that extends up to  $\theta_{obs} \sim 15^\circ$ , with its maximum intensity near the direction of the ion specular reflection, while in metals the maximum was observed at  $\theta_{obs} \sim 10^\circ$ .

Almost all of the models presented to describe the structure at  $E_m$  are based on the interaction of the convoy electron with the induced electric field ( $E_{ind}$ ). A simple description of this effect<sup>7,8</sup> assumes an electron wave packet centered at and moving away with the ion. The kinetic energy of this convoy electron is  $\sim E_{ce}$  when just leaving the region of projectile closest approach to the surface. If the direct electron-projectile interaction is turned off, the change in the convoy electron energy could be directly related to the mechanical work performed by  $E_{ind}$ . The simplicity of this picture is destroyed by the interaction with the projectile; nevertheless we may expect a similar effect to appear on the mean energy of the final electron distribution. For insulator surfaces we also have to consider the track potential: each single ion trajectory leaves behind a microscopic charge density that corresponds to the holes in the valence band and core states produced during the surface ionization. From our measurements as a function of  $I_c$  we can estimate that the decaying time of the track is  $\geq 10^{-10}$  sec, corresponding to the average time between ion impacts for  $I_c \sim 2$  nA, i.e., the critical current below which the macroscopic charge effects disappeared. This is enough time for an electron with velocity close to that of the projectile ( $v_p = 1.5-2$  au in our case) to escape from the surface region. Therefore, the electrons ejected from LiF can feel this attractive potential during all the outgoing trajectory. It is important to observe that the total charge distribution generated by the surface ionization adds up to zero net charge if we account for the emitted electrons.

Contrary to the case of gaseous targets where the projectile-Coulomb potential dominates in the asymptotic region and fixes the electron peak maximum at the projectile velocity, in grazing ion-surface collisions the projectile image potential reduces the electron-projectile interaction to a dipole potential and the characteristic cusp-shaped peak at  $v_p$  is no longer observed.<sup>9,11</sup> Near the surface of the insulator, the interaction of the convoy electron with the track and its ionization electrons can prevail over the dipole potential of projectile plus image charge, shifting the electron energy distribution to lower energies.

To estimate the track potential we calculate, using a first-order semiclassical approximation, the  $F^-$  ionization probabilities in single collisions with  $H^+$  as a function of the impact parameter ( $\rho$ ). The  $\rho$  distribution is determined from classical calculations by assuming grazing  $H^+$  trajectories along random surface directions. For  $E_p = 100$  keV we obtain that  $\sim 10$  electrons are excited to the conduction band during the grazing collision; at least half of them are emitted into the solid, where they are rapidly screened. From the surface ionization probability, we define an average distance between ionization events along the trajectory ( $d_I$ ). The track potential so defined is used to study the evolution of an electron that starts to move in the neighborhood of the ion. The time evolution of the convoy electron and the ionization electrons was described with classical dynamics. The Coulombic interaction among the electrons was taken into account, and the effect of an external potential generated by the moving projectile and the effective positive charges of the

ionized  $F^-$ . The ionization electrons were initially distributed in space according to the electron density of the  $2p F^-$  orbital that originates them. We studied the evolution of a convoy electron produced in a previous projectile-surface interaction. The model uses classical dynamics to describe the interaction of the convoy with the ionized electrons and the track of positive charges produced by the projectile along the outgoing glancing trajectory. The stories considered are those of convoy electrons with energies close to the continuum threshold ( $\sim 2$  eV from this). The potential induced by the convoy-projectile pair polarization of the surface is not included in this preliminary calculation.

The first interesting result obtained from the simulation is that the track potential acting on the convoy electron is equivalent to an attractive potential (net positive charge effect). An electron ejected from a  $F^-$  leaves the surface region with a kinetic energy larger than the potential energy provided by the residual F atom. Except when it is ejected in the forward direction and close to the projectile, it leaves the surface region much faster than the convoy electron or the projectile. The track potential produces a net slowing-down effect on the convoy electron along its outgoing path. The ionized electrons will produce on the average the opposite effect of accelerating the convoy, but this is expected to be weaker for three reasons: (1) the intensity of the electron-electron repulsion is reduced because the ionized electron is moving fast away from the surface; (2) the ionization is produced with nonzero probability in all directions, and the net acceleration effect is reduced to its projection along the convoy outgoing direction of motion; (3) the repulsion between electrons is transformed into equal amounts of kinetic energy to each electron, while the attractive potential between the convoy electron and the residual charge in the surface is mainly transferred (assuming a large effective mass for the hole in the  $F^-$ ) to the convoy kinetic energy; therefore, the slowing-down effect of the later prevails over the acceleration of the former. A similar effect was recently reported for 5 MeV/amu  $Ar^{16+}$  collisions with polypropylene foils.<sup>15</sup> A feature that arises from the net slowing down is that the convoy electrons that start their evolution behind the projectile increase, on the average, their relative velocity ( $v'$ ), and so remain in the continuum having a mean velocity in the laboratory system smaller than  $v_p$ . On the other hand, electrons starting ahead of the projectile undergo a reduction of  $v'$ , falling mainly into bound states. Consequently, the convoy peak distribution moves in space behind the projectile, and the projectile-induced electric field that acts on the trailing electron distribution has a reduced component parallel to the surface. Their acceleration effect is therefore weakened when compared with the case of a metal surface.

In Fig. 3 we present the results obtained for a projectile with  $v_p = 2$  au ( $E_p = 100$  keV). The simulation considers a proton-surface distance of 3 au,<sup>16</sup> and the convoy electrons uniformly distributed in the plane of the projectile trajectory. Typically,  $10^4$  stories were calculated for each projectile initial height above the surface. Three subsequent  $F^-$  ionizations (separated by  $d_I$ ) are considered before the interaction with the surface is turned off. The electron trajectories are followed during 1000 au of time after the last ionization event. Figures 3(a)-3(c) show partial electron energy distributions obtained for convoy electrons starting their trajectory

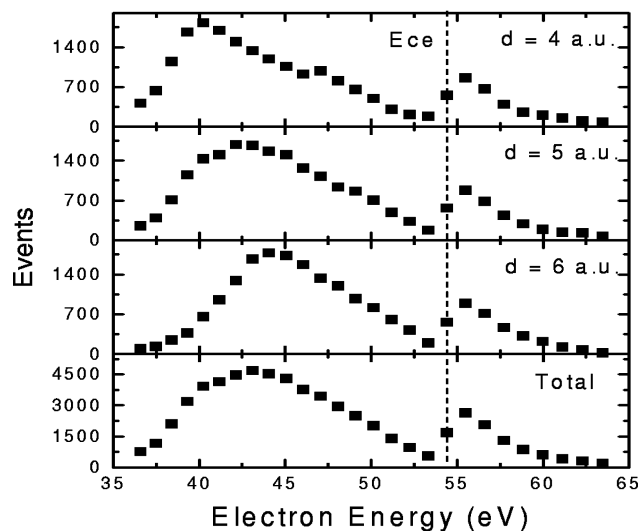


FIG. 3. (a)–(c) Calculated final electron-energy distributions for different initial positions ( $d$ ) of the convoy electrons above the surface. (d) Addition of distributions (a)–(c).

ries at different heights ( $d$ ) from the surface. The separation distance  $d_I$  and the number of ionizations were not critical to determine the shape and position of these distributions. Simulations starting with the proton closer to the surface ( $\leq 2$  au) indicate that the interaction of the convoy electron with the track and its ionization electrons is very strong in this region, producing a spreading out of the convoy electrons. This effect should be enhanced if the binary interactions between convoy electron and the other electrons of the solid were considered. We can see in this figure that all the distributions are shifted to energies lower than  $E_{ce}$ , and that

the shift increases with decreasing  $d$ , i.e. electrons starting closer to the surface are more affected by the track potential. In Fig. 3(d) we show the sum over distributions (a)–(c). Although this result is dependent on the initial population at  $d$ , which is not known, there is certainly a net attractive effect caused by the surface ionization. The  $\Delta E$  observed in the figure is comparable to that measured for the rough surface (A), and larger than that observed for the smooth surface (B). In this case, the repulsive effect of  $V_{ind}$ , not taken into account in this preliminary calculation, will reduce the total-energy shift.

In summary, the energy distributions of electrons emitted forwardly in grazing 60–100 keV  $H^+$ -LiF collisions present a broad structure with its maximum at an energy  $E_m < E_{ce}$ . The experimental results are discussed in terms of the long recombination time of the excess of positive charge produced along the projectile path, which results in a deceleration of the convoy electron distribution. Taking into account that for rough surfaces: (i) the effect of  $V_{ind}$  is diminished and (ii) the target ionization may be enhanced due to an average reduction in the impact parameter distribution, we consider that the greater  $\Delta E$  shifts observed for LiF sample A (in comparison with sample B) are related to the differences in the surface roughness. Although a deeper theoretical study is needed to evaluate the competitive effects of  $V_{ind}$  and  $V_{track}$  along the electron outgoing trajectory, this preliminary calculation suggests that the attractive track potential is responsible for the negative shift  $\Delta E$  observed.

We acknowledge useful discussions with M.L. Martiarena, A. Borisov, and N. Stolterfoht, and partial financial support from CONICET (Grant No. PMT-PICT0437) and Coopertativa de Electricidad Bariloche.

\*Also at Consejo Nacional de Investigaciones Científicas y Técnicas, Argentina.

<sup>1</sup>J. Schou, in *Ionization of Solids by Particles*, Vol. 306 of *NATO Advanced Study Institute Series B: Physics*, edited by R. A. Baragiola (Plenum Press, New York, 1993).

<sup>2</sup>J. Cazaux, in *Ionization of Solids by Particles* (Ref. 1).

<sup>3</sup>C. Auth, T. Hecht, T. Igel, and H. Winter, *Phys. Rev. Lett.* **74**, 5244 (1995).

<sup>4</sup>W. Koning, K. H. Krebs, and Rogaschewski, *Int. J. Mass Spectrom. Ion Phys.* **16**, 243 (1975).

<sup>5</sup>M. Vana, F. Aumayr, P. Varga, and H. P. Winter, *Europhys. Lett.* **29**, 55 (1995).

<sup>6</sup>L. F. de Ferrariis and R. Baragiola, *Phys. Rev. A* **33**, 4449 (1986).

<sup>7</sup>A. Koyama, *Nucl. Instrum. Methods Phys. Res. B* **67**, 103 (1992).

<sup>8</sup>K. Kimura, M. Tsuji, and M. Mannami, *Nucl. Instrum. Methods Phys. Res. B* **79**, 33 (1993).

<sup>9</sup>E. A. Sánchez, O. Grizzi, M. L. Martiarena, and V. H. Ponce, *Phys. Rev. Lett.* **71**, 801 (1993).

<sup>10</sup>G. R. Gómez, E. A. Sánchez, O. Grizzi, M. L. Martiarena, and V. H. Ponce, *Nucl. Instrum. Methods Phys. Res. B* **122**, 171 (1997).

<sup>11</sup>H. Winter, P. Strohmeier, and J. Burgdörfer, *Phys. Rev. A* **39**, 3895 (1989).

<sup>12</sup>C. O. Reinhold, J. Burgdörfer, K. Kimura, and M. H. Mannami, *Phys. Rev. Lett.* **73**, 2508 (1994).

<sup>13</sup>J. E. Gayone, R. G. Pregliasco, G. R. Gómez, E. A. Sánchez, and O. Grizzi, *Phys. Rev. B* **56**, 4186 (1997).

<sup>14</sup>G. R. Gómez, E. A. Sánchez, and O. Grizzi, *Phys. Rev. B* **57**, 12 573 (1998).

<sup>15</sup>G. Xiao, G. Schiwietz, P. L. Grande, A. Schmoltd, M. Grether, R. Köhrbrück, N. Stolterfoht, A. Spieler, and U. Stettner, *Nucl. Instrum. Methods Phys. Res. B* **115**, 215 (1996).

<sup>16</sup>M. Hasegawa, T. Uchida, K. Kimura, and M. Mannami, *Phys. Lett. A* **145**, 182 (1990).